$$\boldsymbol{A} = \frac{\mu}{4\pi} \oint_C \frac{I}{r}\, d\boldsymbol{s} \qquad (6)$$

In the finite element method, this vector potential $\boldsymbol{A}$ was analyzed first of all.

And then from Maxwell's equations (1) to (4), the electric flux density D, charge ρ, electric field strength E, magnetic field strength H, current density J are obtained like this.

$$\mathrm{rot}\ \boldsymbol{A} = \begin{vmatrix} \boldsymbol{i} & \boldsymbol{j} & \boldsymbol{k} \\ \frac{\partial}{\partial x} & \frac{\partial}{\partial y} & \frac{\partial}{\partial z} \\ A_x & A_y & A_z \end{vmatrix}$$

$$B_x = \frac{\partial A_z}{\partial y} - \frac{\partial A_y}{\partial z}$$

$$B_y = \frac{\partial A_x}{\partial z} - \frac{\partial A_z}{\partial x}$$

$$B_z = \frac{\partial A_y}{\partial x} - \frac{\partial A_x}{\partial y}$$

2.3 Building models used for the analyses

As a building model used for the analyses, a symmetric model 1 and an asymmetric model 2 were used.

Model 1 is a simple two-story reinforced concrete building using 22 mmφ steel bar with a width and depth of 7.2 m, and a height is 9.5 m.

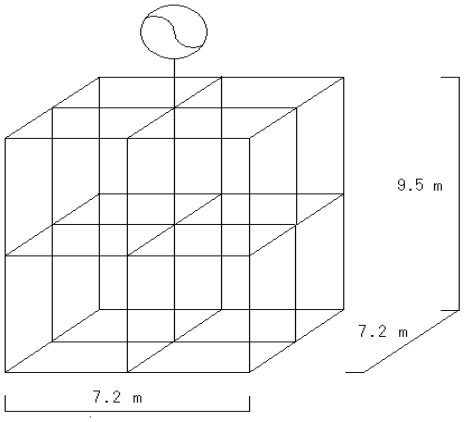

Fig. 1 Model 1 building

Model 2 is a five-story steel frame building using 250 mm × 250 mm steel frame with a transformer room installed on the rooftop. The width and depth of the building are 20 m, the height of each floor is 5 m.

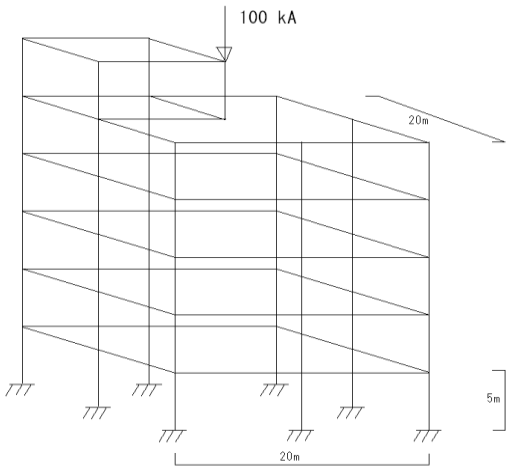

Fig. 2 Model 2 building

For model 2 building, instead of the conventional lightning protection method, we also examined the mesh method [13].

3. Analyzed results on model 1 building

3. 1 Current distribution analyzed result by FEM

Model 1 is a simple 2-story reinforced concrete building, and the analysis of lightning surge current distribution was performed.

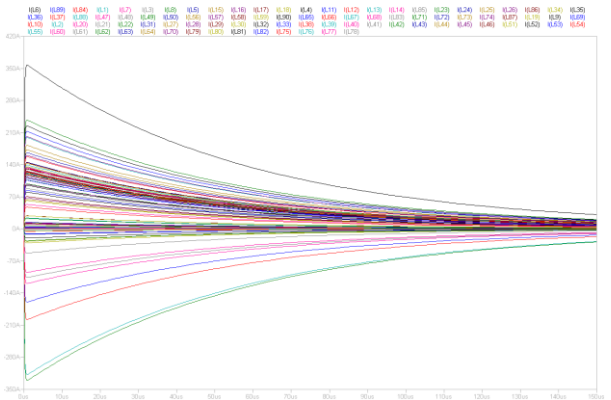

Fig. 3 Lightning surge current distributions inside the model 1 building

Fig. 3 shows a 100kA lightning surge current (1/50 μsec: rise time 1 μsec, half-value width 50 μsec) distributions inside the building. The injection point of the direct lightning surge current having 100kA peak was set at the center of the roof.

Fig. 4 shows a plot of the peak values of the waveforms. In Fig. 4, the currents were the largest at 23.4kA at the central steel bar of the building just below the injection point, 10,9kA at the outer steel bar, and 8.5kA at the corner steel bar. It is considered that this is because the current flows through the shortest path with the lowest impedance.

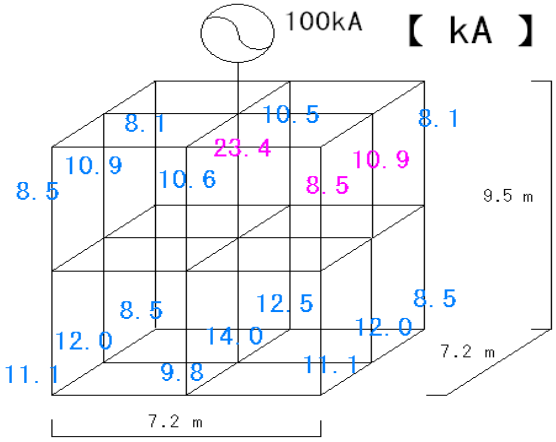

Fig. 4 A plot of the peak values of the waveforms when a 100kA lightning surge current injected into a model 1 building

3. 2 Magnetic field distribution analyzed result by FEM

Furthermore, magnetic field distribution analysis was performed using FEM.

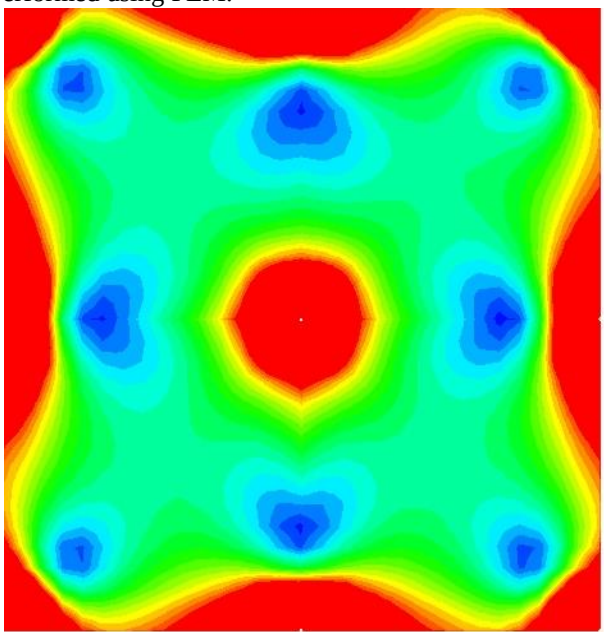

(MAX 2.4×10^{-2} T)

Fig. 5 Magnetic field analyzed result by FEM (Model 1 building: The 2nd floor)

The magnetic field distribution analyzed results on the 2nd and 1st floors using FEM are shown in Figures 5 and 6, respectively.

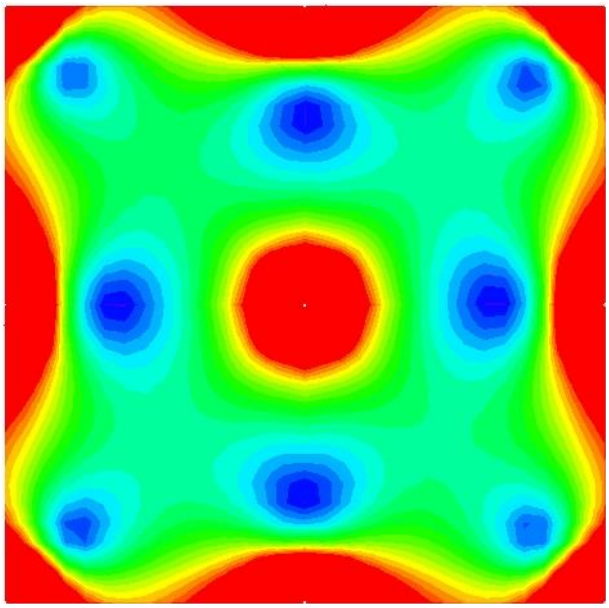

(MAX 2.4×10^{-2} T)

Fig. 6 Magnetic field analyzed result by FEM (Model 1 building: The 1st floor)

In Fig. 5 and Fig. 6, the magnetic field strength of the red part was the strongest, and the magnetic field strength became weaker as the color became orange, yellow, green, blue, indigo, and purple.

Looking at the magnetic field distribution on each floor, the magnetic field distributions on the 1st and the 2nd floors were almost the same. It is considered that this is because the model 1 building is symmetric. In addition, the maximum value of the magnetic field strength on the 1st and the 2nd floors was 2.4×10^{-2} T, which were the same results.

Fig. 7 shows the magnetic field vectors on the 1st floor. Fig. 7 shows that the magnetic field strength was the strongest in the red part of the color, and the magnetic field strength became weaker as the color changes to orange, yellow, green, blue, indigo, and purple.

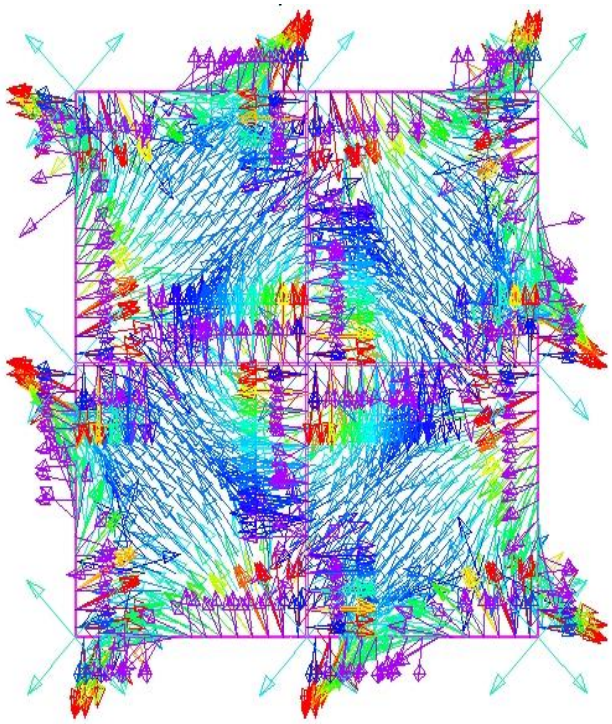

Fig. 7 Magnetic field vector analyzed result by FEM (Model 1 building: The 1st floor)

It was found that the magnetic field vectors are also symmetrical with respect to the magnetic field distribution shown in Fig. 6, and the magnetic field strengths at the center and the edges of the room were large.

From these magnetic field distribution analyzed results, in the case of model 1 building, the center and edges of the room have high magnetic field strength. In other words, in this building model, it became clear that the information systems should be installed in a place away from the center and the edges of the room taking into accout of their immunity levels against magnetic field strength.

4. Analyzed results on model 2 building

4. 1 Current distribution analyzed result by FEM

Fig. 8 shows a plot of the peak values of the waveforms when a 100kA lightning surge current was injected into a model 2 building using FEM. A 35.6kA current flowed through the transformer room which is the injection point. Looking at the left side of the transformer room, current peak values were 21.2kA on the 5th floor, 15.7kA on the 4th floor, 13.9A on the 3rd floor, 13.2kA on the 2nd floor, 12.9kA on the 1st floor.

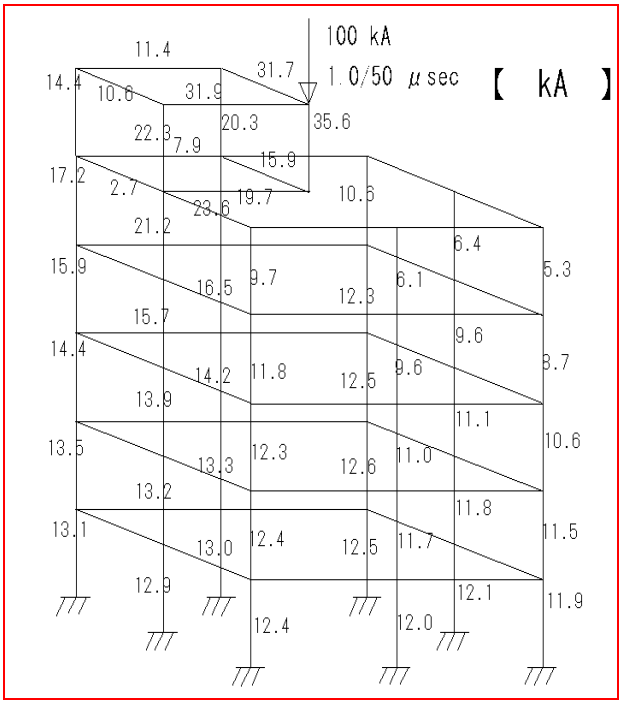

Fig. 8 A plot of the peak values of the waveforms when a 100kA lightning surge current injected into a model 2 building

In addition, looking at the right edge of the buiding, current peak values were 5.3kA on the 5th floor, 8.7kA on the 4th floor, 10.6kA on the 3rd floor, 11.5kA on the 2nd floor, 11.9kA on the 1st floor. They were increased as the floor going down.

4. 2 Magnetic field distribution analyzed result by FEM

The magnetic field analysed results using FEM are shown in Figs. 9 to 13 from the 5th floor to the 1st floor. In Figs. 9 to 13, the magnetic field strength was strongest in the red part, and the magnetic field strength became weaker as the color changes to orange, yellow, green, blue, indigo, and purple.

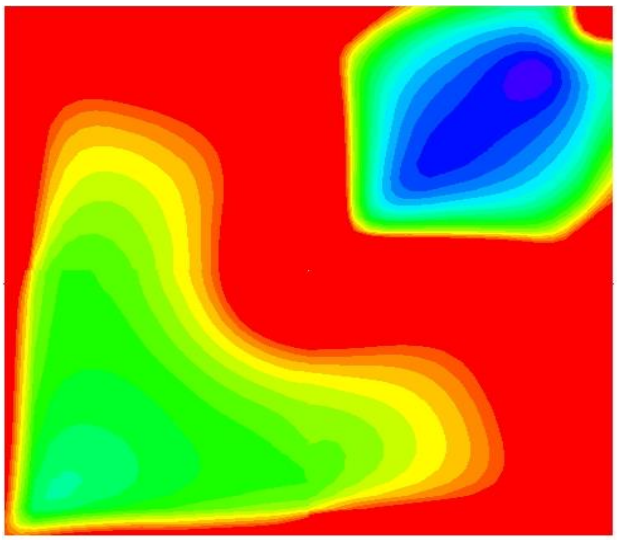

(MAX 3.7×10^{-2} T)

Fig. 9 Magnetic field distribution analyzed result by FEM (Model 2 building:The 5th floor)

Looking at the magnetic field distribution on the 5th floor shown in Fig. 9, the part with the transformer room on the roof had the largest magnetic field strength. The maximum magnetic field strength was 3.7×10^{-2} T.

The maximum magnetic field strength on the 4th floor shown in Fig. 10 was 2.4×10^{-2} T.

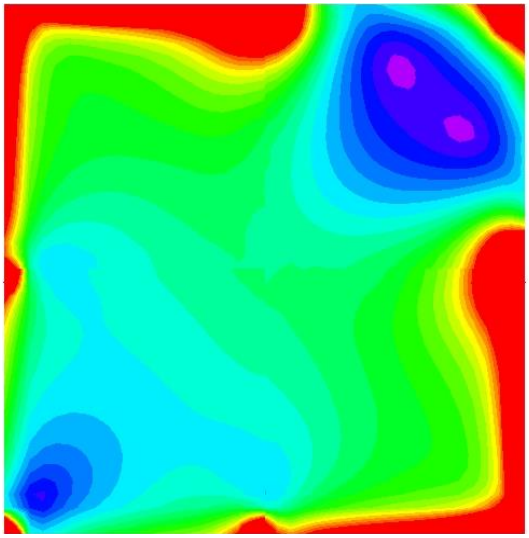

(MAX 2.4×10^{-2} T)

Fig. 10 Magnetic field distribution analyzed result by FEM (Model 2 building: The 4th floor)

The maximum magnetic field strength on the 3rd floor shown in Fig. 11 was 1.7×10^{-2} T.

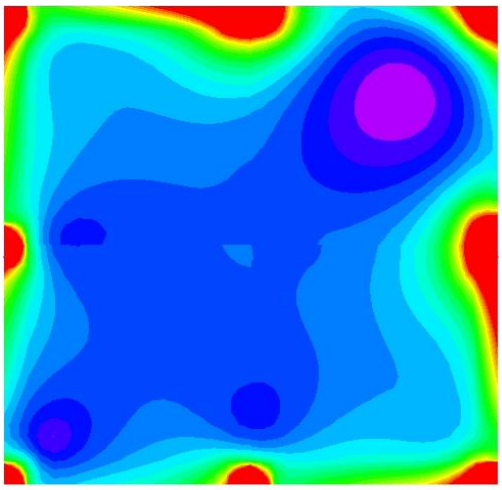

(MAX 1.7×10^{-2} T)

Fig. 11 Magnetic field distribution analyzed result by FEM (Model 2 building: The 3rd floor)

The maximum magnetic field strength on the 2nd floor shown in Fig. 12 was 1.6×10^{-2} T.

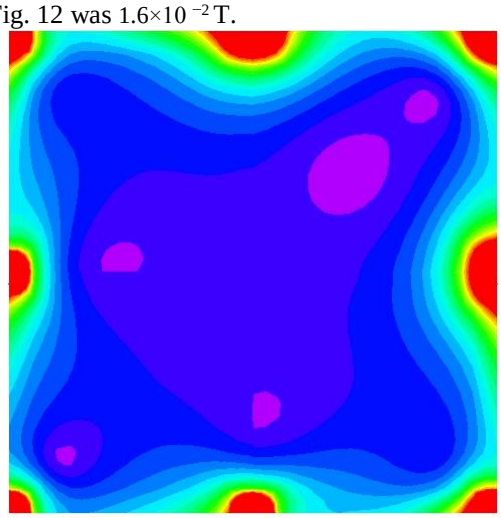

(MAX 1.6×10^{-2} T)

Fig. 12 Magnetic field distribution analyzed result by FEM (Model 2 building: The 2nd floor)

Comparing the magnetic field strength on the 4th floor and the magnetic field strength on the 3rd floor with the magnetic field strength on the 5th floor, it became clear that the magnetic field strengths were weaker by about 30% in the order of the 4th floor and the 3rd floor. It is considered that this is because as the number of floors decreased, the current flowed uniformly through the steel frames and the magnetic fields eliminated each other.

The maximum magnetic field strength of the magnetic field distribution on the 1st floor shown in Fig. 13 was 1.5×10^{-2} T.

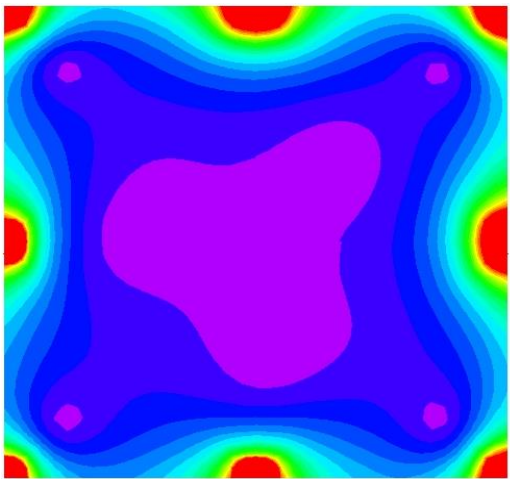

(MAX 1.5×10^{-2} T)

Fig. 13 Magnetic field distribution analyzed result by FEM (Model 2 building: The 1st floor)

Comparison between the second floor shown in Fig. 12 and the 1st floor shown in Fig. 13, the range in which the magnetic field was weakened at the center of the 1st floor.

In other words, in the model 2 building, it was found that it is better to install the information systems at the center of each floor where the influence of the magnetic field is small.

Fig.14 and Fig.15 show the magnetic field vector distribution on the 5th and 1st floors, respectively. Fig.14 and Fig.15 show that the magnetic field strength of the red portion was the strongest, and the magnetic field strength became weaker as the color became orange, yellow, green, blue, indigo, and purple.

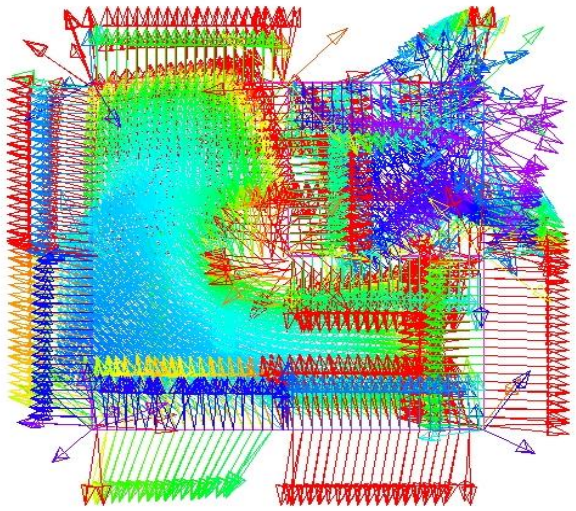

Fig. 14 Magnetic field vector analyzed result by FEM (Model 2 building: The 5th floor)

From the magnetic field vector distribution as shown in Fig.14, the magnetic field vector was asymmetrical on the 5th floor. On the other hand, the magnetic field vector was almost symmetrical on the 1st floor as shown in Fig.15.

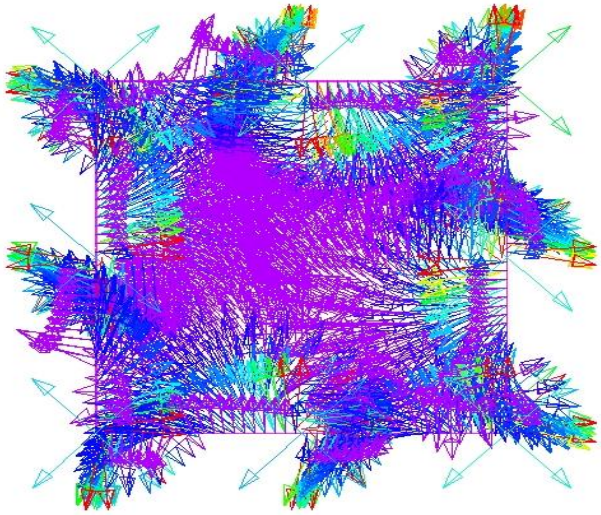

Fig. 15 Magnetic field vector analyzed result by FEM (Model 2 building: The 1st floor)

4. 3 Consideration of current distribution when the mesh method is added to model 2 building

The mesh method is one of the methods for protecting a building from lightning [13].

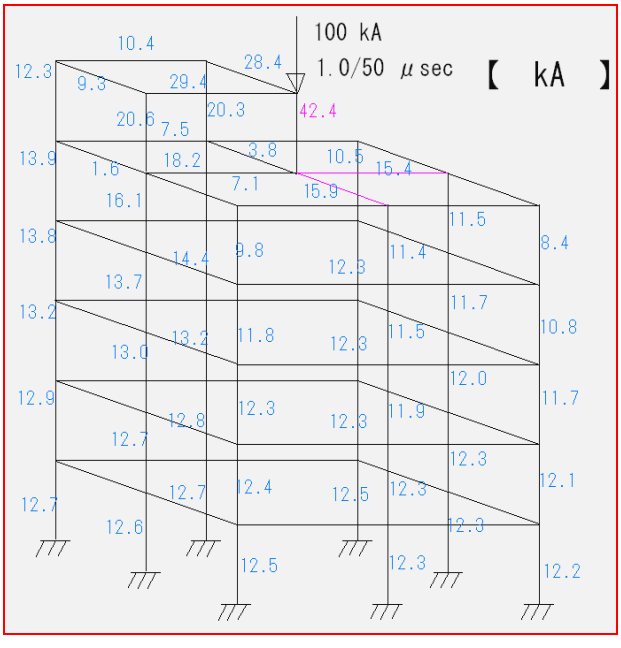

Fig. 16 A plot of the peak values of the waveforms when a 100kA lightning surge current injected into a model 2 building (mesh method is applied)

This method is a new lightning protection method that adds a metal mesh.

In order to confirm the effect of this mesh method, 22 mmφ iron wires were added to the roof of the building model 2 where there was no steel frames (red line portions in Fig. 16) .

Compared with Fig. 8, the value of the current flowing just below the injection point was 35.6 kA, whereas in the model with the added mesh, it increased to 42.4 kA for the same steel frame. It is considered that this is because the impedance just below the injection point decreased.

Also, comparing the current values on the 1st floor, when the mesh method was not applied (Fig. 8), current values were in the range of 11.9 to 13.1 kA. On the other hand, when the mesh method was applied (Fig. 16), the current values were almost uniformly in the range of 12.2 to 12.7 kA on the 1st floor.

Therefore, it became clear that the method of adding iron wires to the part of the roof having no steel frsmes is an effective measure to make the current value uniform.

Conclusion

In this paper, the analyzed results on direct striking lightning surge current and magnetic field distributions inside the buildings using FEM (finite element method) were shown.

(1) As a model used for the analyses, a symmetric model 1 building and an asymmetric model 2 building were used. Model 1 building is a simple two-story model. Model 2 building is a five-story asymmetrical model with a transformer room installed on the rooftop.

(2) In the case of model 1 building, the injection point of the direct lightning surge current having 100kA peak was set at the center of the roof. The currents were the largest at 23.4kA at the central steel bar of the building just below the injection point, 10,9kA at the outer steel bar, and 8.5kA at the corner steel bar. It is considered that this is because the current flows through the shortest path with the lowest impedance.

(3) In the case of model 1 building, as a result of magnetic field analysis, it became clear that information sysytems should be installed in a place away from the center and edges of the room taking into accout of their immunity levels against magnetic field strength.

(4) In the case of model 2 building, A 35.6kA current flowed through the transformer room which is the injection point. Looking at the left side of the transformer room, current peak values were 21.2kA on the 5^{th} floor, 15.7kA on the 4^{th} floor, 13.9A on the 3rd floor, 13.2kA on the 2nd floor, 12.9kA on the 1st floor.

(5)It was also found that in the model 2 building, it is better to install the information sysytems at the center of each floor, which is less affected by the magnetic field.

(6) The mesh method is a new method of lightning protection in which a metal mesh is added. It became clear that the method of adding iron wires to the part of the roof having no steel frames is an effective measure to make the current value uniform.

References

[1] H. Kijima,K.Ochi,Pulse shaping method using bridge tap for fast transient burst test generator, WSEAS Transactions on electronics, Vol.10, pp.94-100, 2019

[2] H. Kijima,T.Hattori,Estimation results on the location error when using cable locator, WSEAS Transactions on systems, Vol.15, pp. 11-18, 2016

[3] K.Takato, H.Kijima, Power line communication degradation caused by surge protective device, IEEJ Transactions on communications, Vol.135, No.2, pp. 181-190, 2015

[4] K.Murakawa, H.Kijima, Earthing resistance tester developed using resonant circuit technology with no auxilliary electrode, WSEAS Transactions on communications, Vol.13 pp. 484-493, 2014

[5] K.Murakawa,H.Kijima, Normalized power spectrum analysis based on LPC using time integral procedure, WSEAS Transactions on communications, Vol.13 pp. 466-475, 2014

[6] H. Kijima,K.Ochi, Proposal of double voltage generator using four coaxial cables, International Journals of circuits, Issue 1, Vol.8, pp. 30-37, 2014

[7] H. Kijima,K.Ochi, High voltage pulse generator using normal cables, WSEAS Transactions on circuits and systems applications, engineering & development, Issue 12, Vol.12 pp. 366-375, 2014

[8] H. Kijima, K.Murakawa, Lightning surge response improvement by combinations of varistors and GDTs, WSEAS Transactions on power systems, Issue 2, vol. 7, pp60-69, 2012

[9] H. Kijima, K.Takato, K. Murakawa, Lightning protection for gas-pipelines installed under the ground, International Journal of systems, Issue 1, vol. 5, pp117-126, 2011

[10] H. Kijima, T. Hasegawa, Electrical force analyzed results on switchgear of disconnector for overvoltage protector, WSEAS Transactions on power systems, Issue 1, vol. 5, pp32-41, 2010

[11] H. Kijima, M. Shibayama, Circuit breaker type disconnector for over voltage protector, WSEAS Transactions on power systems, Issue 5, vol. 4, pp167-176, 2009

[12] H. Kijima, A development of earthing resistance estimation instrument, International Journal of geology, Issue 4, vol. 3, pp112-116, 2009

[13] IEC 62305-3, Protection against lightning, Physical damage to structures and life hazard, 2010

[14] IEC 62305-4, Protection against lightning, Electrical and electronic systems within structures , 2010

[15] M. Sadegh Rahimian, Ali M. Hussein, Calculation of tall-structure lightning current parameters using particle swarm optimization technique, ICLP, pp1-5, 2012

[16] Amedeo Andreotti , Luigi Verolino, A New Channel Base Current Function for Lightning Studies, IEEE Transactions on EMC.Vol. 57, Issue 6, pp1539-1546, 2015

[17] Kok Lian Chia , Ah Choy Liew, Modeling of lightning return stroke current with inclusion of distributed channel resistance and inductance, IEEE Transactions on Power Delivery, Vol.19, Issue 3, pp 1342–1347, 2014

[18] T.Zoltan, Problems of the simulation and modeling the lightning protection of high structures, vol.14, No.2, pp223-234, 2019

[19] T. Shindou, Lightning effects and protection of structures, https://doi.org/10.1002/tee.22649, 2018

[20] S. Shivalli, Lightning effects and protection of structures, IOSR JEEE, Vol.11, Issue 3, pp44-50, 2016